

## Electronic and magnetic properties of FeBr<sub>2</sub>

Z. Ropka

*Center for Solid State Physics, S<sup>nt</sup> Filip 5, 31-150 Krakow, Poland*

R. Michalski

*Center for Solid State Physics, S<sup>nt</sup> Filip 5, 31-150 Krakow, Poland  
and Institute of Physics, Pedagogical University, 30-084 Krakow, Poland*

R. J. Radwanski

*Center for Solid State Physics, S<sup>nt</sup> Filip 5, 31-150 Krakow, Poland  
and Institute of Physics, Pedagogical University, 30-084 Krakow, Poland*

(Received 10 February 2000; revised manuscript received 1 December 2000; published 30 March 2001)

Electronic and magnetic properties of FeBr<sub>2</sub> have been surprisingly well described as originating from the Fe<sup>2+</sup> ions and their fine electronic structure. The fine electronic structure has been evaluated by taking into account the spin-orbit coupling, crystal-field and intersite spin-dependent interactions. The large magnetic moment of iron, of 4.4  $\mu_B$ , can be theoretically derived provided the spin-orbit coupling is explicitly taken into account. These calculations show that for the meaningful analysis of properties of FeBr<sub>2</sub> the spin-orbit coupling is essentially important and that the orbital moment (0.74  $\mu_B$ ) is largely unquenched (by the off-cubic trigonal distortion in the presence of the spin-orbit coupling).

DOI: 10.1103/PhysRevB.63.172404

PACS number(s): 75.10.Dg, 71.70.Ch, 71.28.+d, 75.30.Mb

FeBr<sub>2</sub> became famous a long time ago as one of the strongest metamagnets.<sup>1,2</sup> At 4.2 K an external field of 3.15 T causes a jump of the magnetization from the almost zero value to a very big value of 110 emu/g.<sup>1,2</sup> This latter value corresponds to 4.4  $\mu_B$  per formula unit (f.u.) and per one Fe atom. This value exceeds a theoretical value of 4.0  $\mu_B$ , expected for the spin-only moment. The explanation for this large magnetic moment has been a challenge for the 3d-magnetism theoreticians. FeBr<sub>2</sub> exhibits the antiferromagnetic (AF) ordering below  $T_N$  of 14.2 K. The appearance of the AF ordering is marked in the specific heat by a very pronounced  $\lambda$ -type of peak.<sup>3,4</sup> The appearance of the AF state is also seen in the temperature dependence of the magnetic susceptibility.<sup>5,6</sup> Properties of FeBr<sub>2</sub> have been described using effective Hamiltonians like the  $S_{\text{eff}}=1/2$  Ising Hamiltonian<sup>7</sup> or the  $S_{\text{eff}}=1$  model with the anisotropic exchange.<sup>7-9</sup> All these approaches neglect the orbital contribution.

We have performed calculations of the Fe<sup>2+</sup>-ion electronic structure taking into account the spin and orbital electronic momenta. In our approach we follow the original idea of Van Vleck<sup>10</sup> that electronic and magnetic properties are largely determined by atomic-like electronic structure, but we have performed extended calculations in the  $|LSL_zS_z\rangle$  basis. In this Brief Report we present results of calculations of electronic and magnetic properties of FeBr<sub>2</sub> with the aim of providing the consistent physical description of zero-temperature properties (e.g., the magnetic-moment value and its direction, the insulating state) as well as temperature dependence of the specific heat and of the paramagnetic susceptibility. It turns out that properties of FeBr<sub>2</sub> are predominantly determined by the low-energy electronic structure of the Fe<sup>2+</sup> ions. The Fe<sup>2+</sup> ion is considered to form the 3d<sup>6</sup> system described by  $S=2$  and  $L=2$  resulting from Hund's

rules.<sup>11,12</sup> The low-energy electronic structure results from the removal of the 25-fold degeneracy of the lowest term <sup>5</sup>D. It turns out that there are 15 localized states within 80 meV, 10 others lying more than 2 eV above. The existence of this fine electronic structure causes strong thermal effects in the temperature course of the specific heat and of the magnetic susceptibility. In fact, we have performed quite similar calculations to those that have been successfully made for the description of rare-earth systems like ErNi<sub>5</sub> (Ref. 13) or NpGa<sub>2</sub>.<sup>14</sup> Of course, the electronic states of the 3d ion are calculated in the completely different way owing to much smaller spin-orbit coupling in 3d ions.

The 25 levels, originated from the <sup>5</sup>D term, and their eigenfunctions have been calculated by the direct diagonalization of the Hamiltonian (1) within the  $|LSL_zS_z\rangle$  base. It takes a form<sup>15,16</sup>

$$H_d = H_{\text{cub}} + \lambda LS + B_0^2 O_0^2 + \mu_B (L + g_s S) B. \quad (1)$$

The separation of the crystal-electric-field (CEF) Hamiltonian into the cubic and off-cubic part is made for the illustration reason as the cubic crystal field is usually very predominant. In the crystallographic structure of FeBr<sub>2</sub> the Fe ion is surrounded by 6 Br ions.<sup>4,6,8</sup> Despite of the hexagonal elementary cell Br ions form the almost octahedral surrounding—it justifies the dominancy of the octahedral crystal field interactions. Moreover, this octahedral surrounding in the hexagonal unit cell can be easily distorted along the local cube diagonal—in the hexagonal unit cell this local cube diagonal lies along the hexagonal  $c$  axis. The related distortion can be described as the trigonal distortion of the local octahedron. The cubic CEF Hamiltonian takes, for the  $z$  axis along the cube diagonal, the form  $H_{\text{cub}} = -\frac{2}{3} B_4 \cdot (O_4^0$

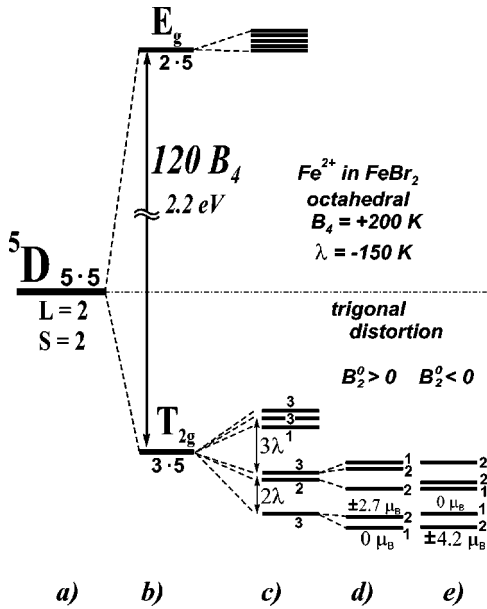


FIG. 1. The fine electronic structure of the highly-correlated  $3d^6$  electronic system. (a) The 25fold degenerated  ${}^5D$  term given by Hund's rules:  $S=2$  and  $L=2$ ; (b) the effect of the cubic octahedral crystal field; (c) the combined action of the spin-orbit coupling and the cubic crystal field:  $B_4 = +200$  K,  $\lambda = -150$  K; (d) and (e) an extra splitting produced by the trigonal distortion—the case (e) is realized in  $\text{FeBr}_2$ ; the trigonal-distortion parameter  $B_2^0 = -30$  K produces a spinlike gap of 2.8 meV.

$-20\sqrt{2}O_4^3$ ), where  $O_m^n$  are the Stevens operators. The last term in Eq. (1) allows studies of the influence of the magnetic field.

The obtained energy level scheme is shown in Fig. 1. These three above-mentioned interactions yield a magnetic doublet ground state with an excited singlet at 33 K, see Fig. 1(e). The degeneracy of the ground doublet is spontaneously removed by the formation of the magnetic state. In the ordered state occurring below 14.2 K the molecular field is set up self-consistently as  $B = -n\langle m_d \rangle$ , where  $n$  is the molecular-field coefficient and  $m_d = -\mu_B(L + g_s S)$ . It originates from intersite spin interactions. Thus our full Hamiltonian for  $\text{FeBr}_2$  contains two, intra- and interion, terms:

$$H = \sum H_d + \sum H_{d-d}, \quad (2)$$

where  $H_{d-d}$  can be written as<sup>13,14</sup>

$$H_{d-d} = \sum \sum n \left( m_d \langle m_d \rangle - \frac{1}{2} \langle m_d \rangle^2 \right). \quad (3)$$

The last term in Eq. (3) is included in order to avoid the double counting (see, for instance Refs. 13 and 14). This intersite interactions produce the magnetic state; in case of  $\text{FeBr}_2$  it is antiferromagnetic arrangement (along the  $c$  axis) of the ferromagnetic planes ( $\perp c$ ).

The  $d$ -electron specific heat is calculated by making use of the general formula<sup>13,14</sup>  $c_d(T) = -T[\delta^2 F(T)/\delta T^2]$ , where  $F(T)$  is the free energy calculated over the available energy

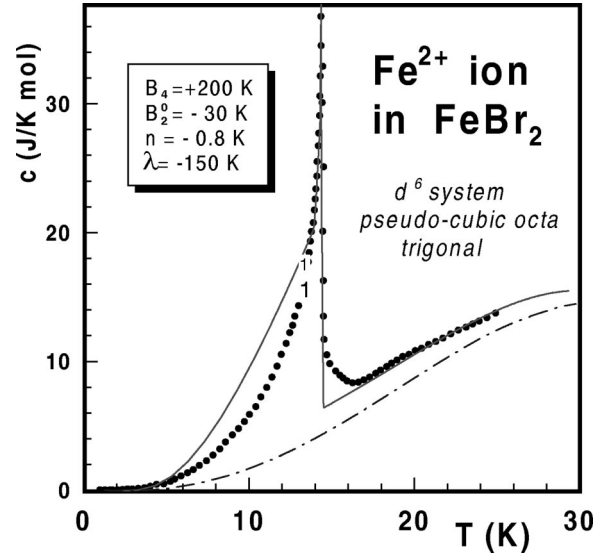


FIG. 2. The calculated temperature dependence of the specific heat of  $\text{FeBr}_2$  (the solid line) as composed from the lattice contribution, shown by the dashed-point line, and the  $d$ -electron contribution with the  $\lambda$  peak at  $T_N$ . Points represent experimental data after Ref. 3.

states resulting from the consideration of the Hamiltonian (1), with Eq. (3) if the magnetically-ordered state is realized. Similarly, the paramagnetic susceptibility  $\chi_d(T)$  can be evaluated.

Results for the temperature dependence of the specific heat  $c_d(T)$  and of the magnetic susceptibility  $\chi_d(T)$  of the  $\text{Fe}^{2+}$ -ion system are shown in Figs. 2 and 3, respectively. The parameters used are as follows:

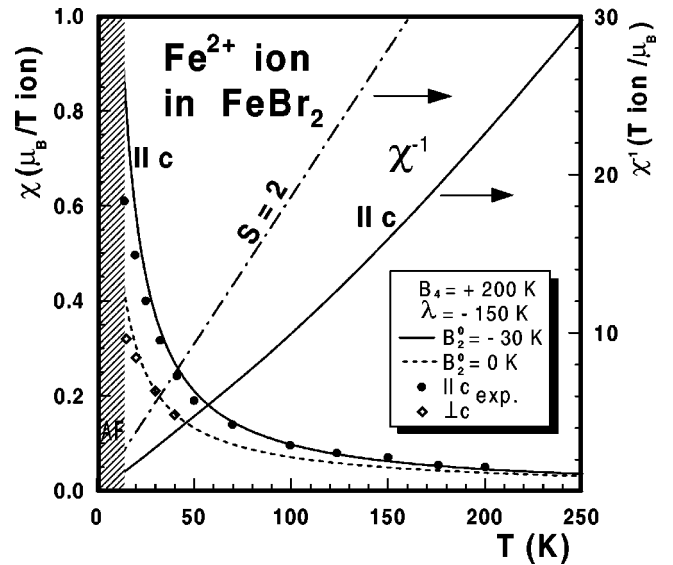


FIG. 3. The calculated temperature dependence of the paramagnetic susceptibility of the  $\text{Fe}^{2+}$  ion in the slightly-distorted octahedral crystal field (the solid line). The dashed line shows the susceptibility for the exactly octahedral crystal field and the spin-orbit coupling. Points represent experimental data for  $\text{FeBr}_2$  (Ref. 6, p. 58).

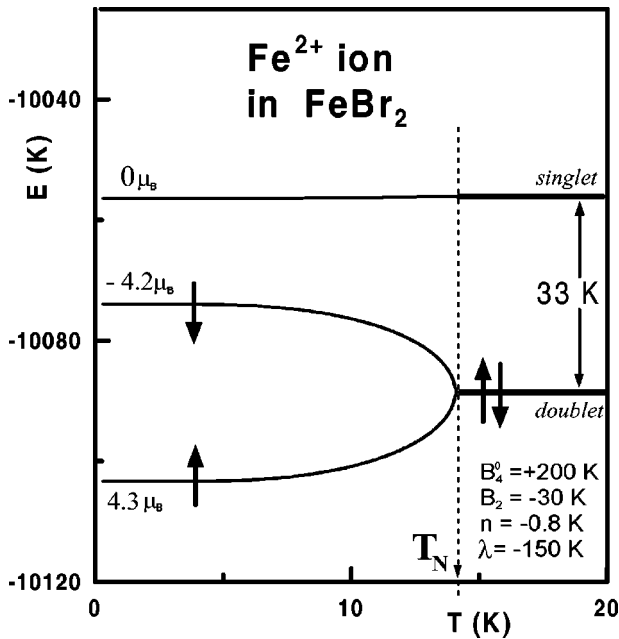


FIG. 4. Temperature dependence of the three lowest levels showing the splitting of the lowest doublet in the magnetic state (below  $T_N=14.2$  K). The collapse of the splitting of the ground-state doublet should be noticed.

(1) The cubic  $B_4$  parameter is taken as  $+200$  K in order to get the overall crystal-field splitting  $E_g-T_{2g}$  of about  $2$  eV ( $=120 \cdot B_4$ )—such splitting explains the yellow color of  $\text{FeBr}_2$ ; this splitting is visible also in optical measurements; (2) the spin-orbit coupling  $\lambda$  equals  $-150$  K as is given for the  $\text{Fe}^{2+}$  ion in Ref. 15 on p. 399; (3) the trigonal distortion  $B_2^0 = -30$  K yields the singlet-doublet splitting of  $D=33$  K ( $2.8$  meV) with the doublet lower, see Fig. 1(e); (4) the molecular-field coefficient  $n = -0.8$  K/ $\mu_B^2$  ( $= -1.2$  T/ $\mu_B$ ) has been adjusted in order to reproduce the experimentally observed Néel temperature of  $14.2$  K.

All these parameters are physically very reasonable. The cubic CEF is responsible for the large energy scale (say,  $1.5$ – $4.0$  eV) and the spin-orbit coupling for the medium,  $25$ – $200$  meV, energy scale. The off-cubic distortion causes energetical effects up to  $10$ – $15$  meV. The magnetic interactions range up to, say,  $20$  meV for compounds with the high magnetic ordering temperature. In case of  $\text{FeBr}_2$  they are of  $1.5$  meV only. The inclusion of the relatively weak intersite magnetic  $H_{d-d}$  interactions is indispensable for the appearance of the long-range magnetic order. They cause an internal magnetic field, of  $5.15$  T at  $0$  K, and a Zeeman-like splitting of the doublet levels. The splitting is strongly temperature dependent and it diminishes at  $T_N$ . The temperature dependence of the three lowest levels is shown in Fig. 4. These three levels with their temperature dependence are responsible for the low-temperature specific heat. In fact, the  $\lambda$ -peak dependence is mainly determined by the temperature dependence of the lowest level. Of course, the temperature dependence occurs only in the magnetically-ordered state as the temperature dependence of the CEF levels, if exist, is expected to be negligible provided the crystallographic structure is not changed.

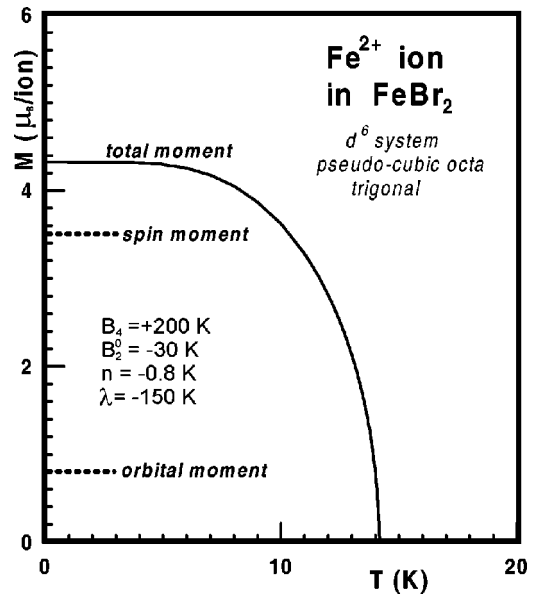


FIG. 5. The calculated temperature dependence of the local magnetic moment of the  $\text{Fe}^{2+}$  ion in  $\text{FeBr}_2$  together with spin and orbital contributions at  $0$  K.

The magnetic-moment value is perfectly reproduced by our calculations. We have obtained a value of  $4.26 \mu_B$  in very good agreement with experimental data.<sup>1,2</sup> The moment is directed along the hexagonal  $c$  axis that is the natural distortion direction. Such the direction provides the Ising-like behavior of the  $\text{Fe}^{2+}$  ion moment, seen in the magnetization curves. The present approach allows for the evaluation of the orbital and spin contributions; see Fig. 5. The  $S_z$  value amounts to  $+1.74$  (the spin moment of  $3.48 \mu_B$ ) whereas the calculated orbital moment amounts to  $0.78 \mu_B$ . It is very large—it amounts to  $18\%$  of the total moment. (On the other hand sceptists can say that it is only  $39\%$  of the full orbital moment of  $2 \mu_B$ .) These studies about the magnetic-moment value and the different effects on the fine electronic structure indicate that the orbital moment has to be “unquenched” in the solid-state physics.

This large orbital contribution is also seen in the temperature dependence of the paramagnetic susceptibility. The effective moment of  $5.39 \mu_B$ , calculated from the  $\chi^{-1}$  vs  $T$  plot at room temperature, exceeds by  $11\%$  the spin-only moment with  $S=2$ . Our calculated effective moment is in very good agreement with typical values often found in  $\text{Fe}^{2+}$ -ion compounds (Ref. 11, Table 14.2; Ref. 12, Table 31.4). Such the increase is attributed in the effective approaches to the change of the  $g$  factor; instead of  $2$  it would be  $2.22$ . It means that our approach allows the calculation of the spectroscopic  $g$  factor that is in good agreement with experimental data.

The found molecular-field coefficient  $n$  of  $1.2$  T/ $\mu_B$ , determining the magnetic-ordering temperature, indicates that  $2/3$  of it is related with antiferromagnetic interactions as a value of  $0.8$  T/ $\mu_B$  is derived from the metamagnetic field of  $3.15$  T.

In conclusion, temperature dependence of the specific heat and of the magnetic susceptibility of  $\text{FeBr}_2$  as well as the zero-temperature magnetic moment and its direction have

been surprisingly well described as originating from low-energy localized states of the  $\text{Fe}^{2+}$  ions. The present approach provides the consistent physical description of the electronic structure in the 0–4 eV energy range. The obtained good agreement indicates that the six 3d electrons in the  $\text{Fe}^{2+}$  ion fulfills the Russel-Saunders scheme and two

Hund's rules quite well. These calculations show that for the meaningful analysis of electronic and magnetic properties of  $\text{FeBr}_2$  the spin-orbit coupling is essentially important and that the orbital moment is largely "unquenched" (by the off-cubic trigonal distortion in the presence of the spin-orbit coupling).

- 
- <sup>1</sup>M.K. Wilkinson, J.W. Cable, E.O. Wollan, and W.C. Koehler, *Phys. Rev.* **113**, 497 (1959).
- <sup>2</sup>L.S. Jacobs and P.E. Lawrence, *Phys. Rev.* **164**, 866 (1967).
- <sup>3</sup>M.C. Lanusse, P. Carrara, A.R. Fert, G. Mischler, and J.P. Redoules, *J. Phys. (Paris)* **33**, 429 (1972).
- <sup>4</sup>H. Aruga Katori, K. Katsumata, and M. Katori, *Phys. Rev. B* **54**, R9620 (1996).
- <sup>5</sup>Y. Bertrand, A.R. Fert, and J. Gelard, *J. Phys. (Paris)* **35**, 385 (1974).
- <sup>6</sup>K. Katsumata, in *Magnetic Properties of Halides*, edited by H.P.J. Wijn, Landolt-Börnstein New Series, Group III, Vol. 27j1 (Springer-Verlag, Berlin, 1994), p. 1.
- <sup>7</sup>M. Pleimling and W. Selke, *Phys. Rev. B* **56**, 8855 (1997).
- <sup>8</sup>K. Katsumata, H. Aruga Katori, S.M. Shapiro, and G. Shirane, *Phys. Rev. B* **55**, 11 466 (1997).
- <sup>9</sup>R.J. Birgeneau, W.B. Yelon, E. Cohen, and J. Makovsky, *Phys. Rev. B* **5**, 2607 (1972).
- <sup>10</sup>J. Van Vleck, *The Theory of Electric and Magnetic Susceptibilities*, (Oxford University, New York, 1932).
- <sup>11</sup>C. Kittel, *Introduction to Solid State Physics* (Wiley, New York 1996), Chaps. 14 and 15.
- <sup>12</sup>N.W. Ashcroft and N.D. Mermin, in *Solid State Physics* (Academic, New York, 1976), Chap. 31.
- <sup>13</sup>R.J. Radwanski, N.H. Kim-Ngan, F.E. Kayzel, J.J.M. Franse, D. Gignoux, D. Schmitt, and F.Y. Zhang, *J. Phys.: Condens. Matter* **4**, 8853 (1992).
- <sup>14</sup>R.J. Radwanski, *J. Phys.: Condens. Matter* **8**, 10467 (1996).
- <sup>15</sup>A. Abragam and B. Bleaney, *Electron Paramagnetic Resonance of Transition Ions* (Clarendon, Oxford, 1970).
- <sup>16</sup>R.J. Radwanski and Z. Ropka, cond-mat/9907140 (unpublished).